Effects of Sliding Velocity and Thermal Conduction of the Tool on X20Cr4 Steel Friction Coefficient and Structure in Nanostructuring Burnishing

IOP Conf. Series: Journal of Physics: Conf. Series **1045** (2018) 012002 doi:10.1088/1742-6596/1045/1/012002

Effects of Sliding Velocity and Thermal Conduction of the Tool on X20Cr4 Steel Friction Coefficient and Structure in Nanostructuring Burnishing

V P Kuznetsov, A S Skorobogatov, M L Lobanov, A S Yurovskih, M S Khadyev, M S Karabanalov

Institute of New Materials and Technologies, Ural Federal University, 28 Mira St., 620078 Ekaterinburg, Russia

E-mail: v.p.kuznetcov@urfu.ru

Abstract. The developmental study has succeeded in finding how the sliding velocity of an indenter affects the friction coefficient and changes the structure and phase state in the surface layer of a X20Cr13 stainless steel when nanostructuring burnishing is done with a tool with no heat removal and, alternatively, when the tool is equipped with a cooling system. It has been shown that structural dispersion of the treated material results in obtaining 20…80 nm nanocrystallites if the friction coefficient of the spherical synthetic diamond indenter is within 0.15…0.18 nm. Application of a compact cooling system, based on Peltier's thermoelectric module, made it possible to stabilize the friction coefficient at 0.17 and to increase the sliding velocity from 13 m/min, this being the case of no heat removal, to 45 m/min in the case when the cooling system having a cooling performance of 120 W was used. TEM and SEM analyses of the surface layer structure confirmed that there is a correlation between the friction coefficient and the size of nanocrystallites and the thickness of the dispersed layer. EBSD analysis of the structure showed that a maximum permissible sliding velocity can be established as referenced to the nucleation and growth of γ-phase grains in the nanostructured layer caused by heating of the material under deformation and reaching the temperature beyond the point α'→γ phase transition as well as by behavior of dynamic recrystallization. It was established that the heat removal ensures suppression of dynamic recrystallization when the sliding velocity is increased up to 50 m/min.

1. Introduction

Fragmenting the grain structure in structural materials until nanocrystallites are obtained significantly improves their physical, mechanical and functional properties. Nanocrystalline structures are predominantly achieved by severe plastic deformation techniques (SPD) such as multi axial forging, rolling, ECAP, HPT, etc. Consistent results of forming a nanostructural state in the surface layer are yielded by nanostructural burnishing when finishing is done on machines.

Kuznetsov et al. showed that the nanostructural state in a thin surface layer of heat-strengthened structural steels is achieved by applying a sliding spherical indenter with a friction force of 20…70 N in the contact; it ensures obtaining a degree of accumulated deformation of 2…9 [1]. It was established that consistent forming of nanocrystallites measuring 20…50 nm in the surface layer with a thickness up to 8 μm is possible if the sliding velocity is 4…12 m/min. Kuznetsov et al. determined that increasing the velocity beyond 12 m/min results in a considerably lower microhardness, worse

roughness and destruction of the surface layer caused by a loss of the shear stability of the material. Limiting the linear velocity of the sliding indenter can be attributed to changing mechanisms of the contact friction due to friction heat; it brings about higher costs of nanostructural burnishing [2].

Korzynski et al. studied effects of burnishing on the fatigue strength of 42CrMo4 and 41Cr4 chrome-coated steels [3]. Burnishing was done with a spherical indenter. It was proved that sliding burnishing improves smoothing of the surface roughness. What is more, it contributes to reaching a high level of compressing residual stresses which in the case of cyclic symmetrical deflecting gives a better fatigue strength up to 40%. To minimize the friction coefficient and heat emission an indenter with a natural diamond was used. Therefore, no attempts were made to establish the effects of friction loading and thermal state of the material under deformation.

Kuznetsov et al. determined values of the friction coefficient for indenters fitted with PCD synthetic diamonds and DBN cubic boron nitride in tribological tests performed on X20Cr13 and X20Cr4 steels applying a reciprocating pattern at velocities of 0.07 and 0.035 m/s in dry conditions and with lubrication [4]. It was defined that the value of the friction coefficient in the cases of sliding the PCD on X20Cr13 steel and the DBN on X20Cr4 steel was 0.14…0.30 and 0.13…0.17 in dry conditions and ~0.12 and 0.07…0.09 in lubrication, respectively. However, no research was done into determining the friction coefficient and discovering structural transformations in the material at sliding velocities exceeding 0.07 m/s. All the more so, the reciprocating pattern of tribological tests offers no opportunity to simulate real conditions for sliding the indenter simultaneously in the direction of the velocity and the feed of burnishing.

Rabinowicz and Imai researched into the friction of a stainless steel pin on a stainless steel disk coated with low-melting-point materials under gradually increasing temperatures [5]. It was ascertained that there occurs a 1.5…7-fold increase of the friction coefficient when the temperature approaches the melting point of the coating material. The authors associated these abrupt increases of the friction coefficient with a growing effect of adhesion though no consideration was given to alterations of either the phase state, or the structure of the low-melting-point material. What is more, throughout the tests the velocity remained constant standing at 0.1 m/s. Bonnet et al. looked into the effect of the sliding velocity on the friction coefficient of a +TiN coated spherical pin on AISI 316L steel [6]. The research showed that while the sliding velocity is below 60 m/min, the value of the friction coefficient is constant and is equal to 0.4. As the velocity rises beyond this value, the friction coefficient begins to go down until it stabilizes at 0.27 with the velocity being 120 m/min. Similar research was undertaken by Ben Abdelali et al. [7], which demonstrated that the steady values of the friction coefficient were 0.54 and 0.23 at velocities of 60 m/min and 120 m/min respectively. Somehow, the researchers did not take into consideration the heating of the material in the tribological contact as a factor influencing the friction coefficient.

Bonnet et al. [6] and Ben Abdelali et al. [7] also studied branching of frictional heat for a carbide+TiN coated pin sliding on AISI 316L and AISI 1045 steels. They proved that the fraction of heat going into the pin decreases from 22 to 15% and from 60 to 10%, respectively, when the sliding velocity goes over 60 m/min. Meanwhile, they did no research into the correlation between the structural state of the material and the friction coefficient in respect to alterations of the sliding velocity and the pin's thermal state.

From our point of view, dynamic recrystallization of the nanostructured layer is likely to originate resulting from a combined impact of SPD and the temperature, which bring about a critical density of dislocations and the diffusion activity of the material. McQueen and Jonas determined that when active loading is applied, dynamic recrystallization can be observed as soon as the temperatures are $0.3…0.35T_m$ [8]. Pu et al. showed an evolving mechanism of dynamic recrystallization in the case of cryogenic burnishing of an AZ31B magnesium alloy [9]. At the same time, no research was revealed that would have looked into recrystallization of nanostructuring friction finishing of structural steel.

Kuznetsov et al. discovered a possibility to increase the rate of nanostructuring burnishing for X20Cr4 steel utilizing liquid cooling of the tool indenter with a capacity of heat removal ~10 W [10]. Application of a dual-cycle cooling system succeeded in obtaining consistent formation of the surface

layer, its roughness being Ra<170 μm and its microhardness almost reaching ~1200 $HV_{0.5}$ if the sliding velocity of the indenter stayed below 25 m/min. No correlation was investigated between the sliding velocity, on the one hand, and the friction coefficient and the surface layer structure, on the other hand, in the case of applying liquid cooling.

The goal of the present research is to establish patterns representing the changes of the friction coefficient and the structure and phase state in the surface layer of X20Cr13 stainless steel occurring when the sliding velocity of the spherical indenter equipped with a tool cooling system is increased.

2. Experimental setup

The developmental research on nanostructuring burnishing made use of disk-type samples, manufactured of X20Cr13 thermo-strengthened steel (C <0.20, Cr 12.7, Si <1.0, Mn <1.0 Mo 0.69, V 0.22, Fe rest (wt.%)) and having a diameter of 60 mm and a thickness of 12 mm. After hardening at 1050 °C and soaking for 2 hours, followed by low tempering at 150 °C, the material had a lath martensite structure with laths measuring 150…200 nm, its hardness being 45…46 HRC.

The flat surfaces of the samples were machined on a KNUTH V-Turn 410 lathe by cutting and consequent nanostructuring burnishing on two sides. Cutting was done with a Sandvik WNMG 080408-SM carbide insert at a cutting speed of 80 m/min, while the feed was 0.06 mm/rev. After the cutting had been done, the microhardness was 690…750 $HV_{0.5}$. Nanostructuring burnishing of the surfaces followed the scheme presented at (Figure 1, a); it was dry burnishing applying a normal force of 340 N on the indenter F_b, and the tool feed rate was f_b=0.025 mm/rev. As the tool was being fed, the sliding velocity increased linearly from 3 to 75 m/min.

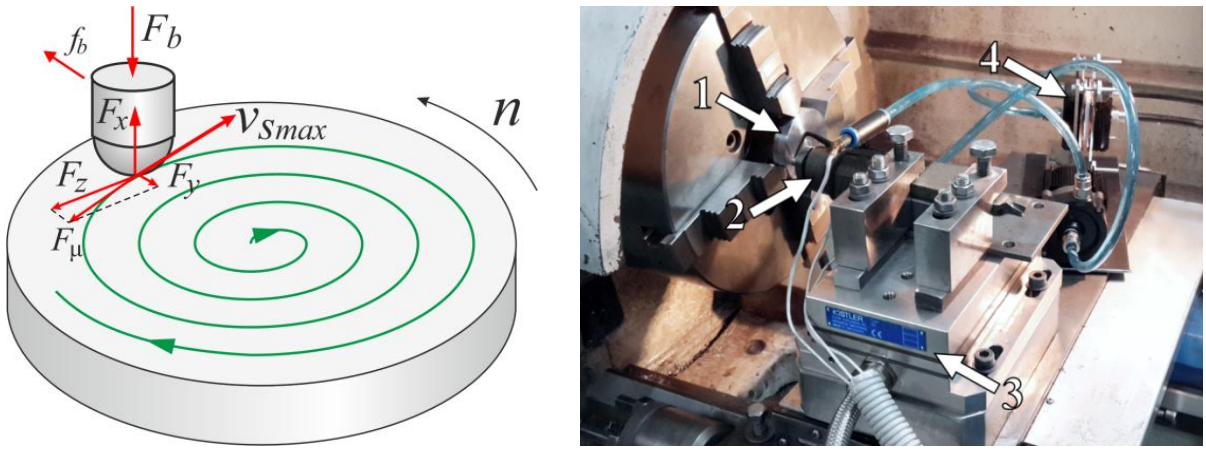

(a) (b)

Figure 1. Machining of the experimental sample: a – kinematic scheme of nanostructuring burnishing; b – photo showing the experimental unit mounted on a KNUTH V-Turn 410 lathe

A special tool was developed that enabled to research into the processing procedure without heat removal and with an indenter cooling system (Figure 2, a). The principle of operation of the cooling system is based on applying the Peltier thermoelectric module (Peltier TEC) with a cooler [10]. Heat is removed from the indenter by a circulating coolant with a pump (pump1) in a closed circuit through special channels in the tool and in the cooler. To maintain a consistent cooling performance of the TEC another loop was integrated into the system for water cooling. Maximum cooling performance primarily depends on the overall dimensions of the tool. The designed tool with a compact cooler enabled to provide a cooling performance of 120 W.

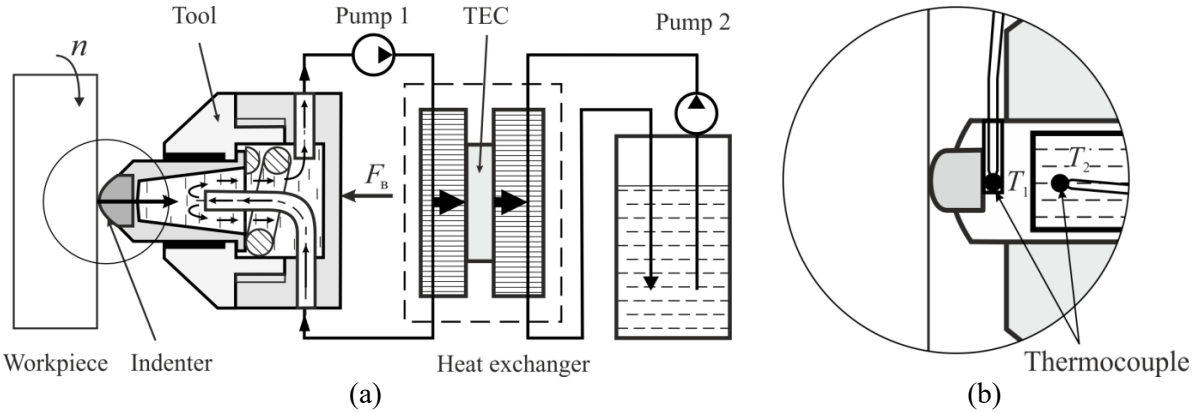

Figure 2. Illustration of the tool dual loop cooling system (a) and the sensing unit (b) for measuring the temperature of the tip and the cooling agent

In the process of the research one face of the sample was burnished by the tool with no heat removal from the indenter, while the other face was done with the tool with the cooling system in operation. The indenters, used for burnishing, were fitted with 2mm radius spherical synthetic diamond tips, the roughness of their working surface being Ra≤0.05 μm. Sample 1 (Figure 1, b) was burnished on the KNUTH V-Turn 410 lathe. Burnishing tool 2 was fitted into a three-axis Kistler 4257BA dynamometer 3. The Peltier module with the cooler 4 was mounted on the slide assembly of the machine. Type K thermocouples were used to measure the temperature T_1 of the indenter tip and the temperature T_2 of the cooling agent circulating in the closed loop (Figure 2, b).

TEM, SEM and EBSD techniques were applied and JEOL JEM 2100 and Zeiss AURIGA CrossBeam microscopes were used for studying the surface layer after finish machining and nanostructuring burnishing had been completed. Microhardness was measured with the Vickers technique on a Leica VMHT microhardness tester applying 0.25 N on the indenter.

3. Results and Discussion

3.1. Friction coefficient and indenter temperature

Dynamometry of nanostructuring burnishing (Figure 3), done with the tool which had no heat removal, showed that a normal force in contact F_x fluctuates with an amplitude of 340±70 N. Application of the indenter cooling system made it possible to reduce the amplitude of these fluctuations to 50 N. Initially at a sliding velocity of 11 m/min the contact force F_z initially goes down from 120 N to 50 N in the case of burnishing with no heat removal with peaks of short duration within 200 seconds of the experiment. As the velocity increases, the force F_z rises in an abrupt to ~100 N, and after 300 seconds it starts to fluctuate again in the range from 50 to 100 N. The fluctuations lead to wearing out the indenter when the total time of the experiment reaches the 370-th second; it corresponds to the sliding velocity v_s≈20 m/min. In the case of applying the indenter cooling system the force F_z is consistent throughout the length of the experiment until the velocity is 75 m/min.

The friction coefficient was calculated making use of the obtained dynamometric data:

$$\mu = \frac{\sqrt{F_y^2 + F_z^2}}{F_x} = \frac{F_\mu}{F_x}, \tag{1}$$

where F_x is normal reaction force; F_y is reaction force in the direction of sliding velocity v_s and F_z is normal reaction force in the direction of feed f_b.

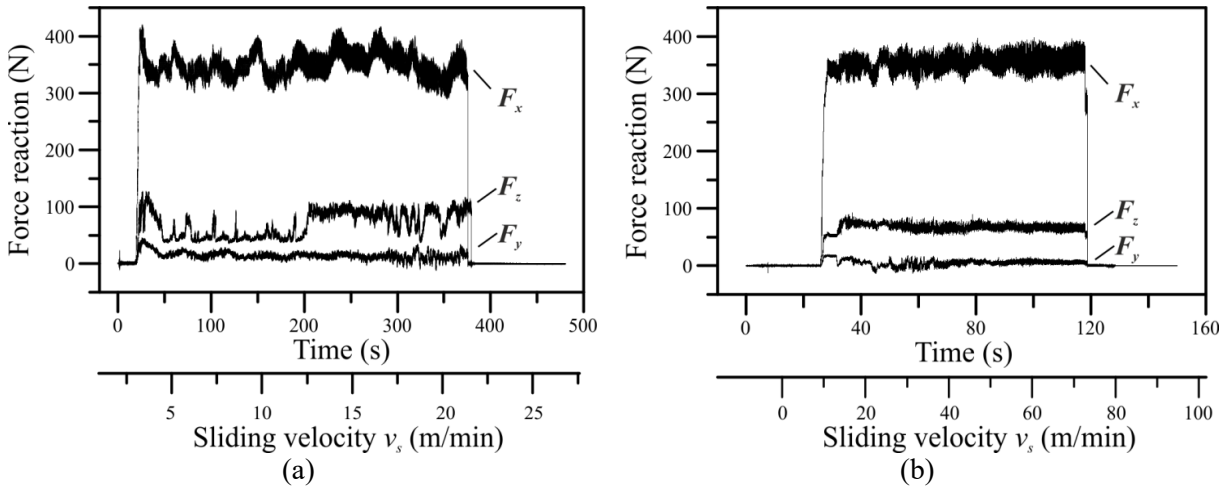

Figure 3. Dynamometry of contact forces in nanostructuring burnishing: a – no heat removal applied; b – cooling system applied.

The pattern of the manner, in which the coefficient of friction changes depending on the value of the indenter sliding velocity, is identical in both cases, for the application with no heat removal and for the other case when the cooling system is in operation (Figure 4). Initially the coefficient of friction goes down reaching the steady-state value μ=0.13 when burnishing with no heat removal and μ=0.17 when burnishing with the cooling system. The steady-state value of the friction coefficient remains until the critical velocity v_{crit} is reached; it is ~13 m/min without heat removal and ~45 m/min in the case of cooling (Table 1). As soon as the critical velocity is exceeded, a sharp increase of the friction coefficient occurs. It starts to go down again when the velocity continues to grow.

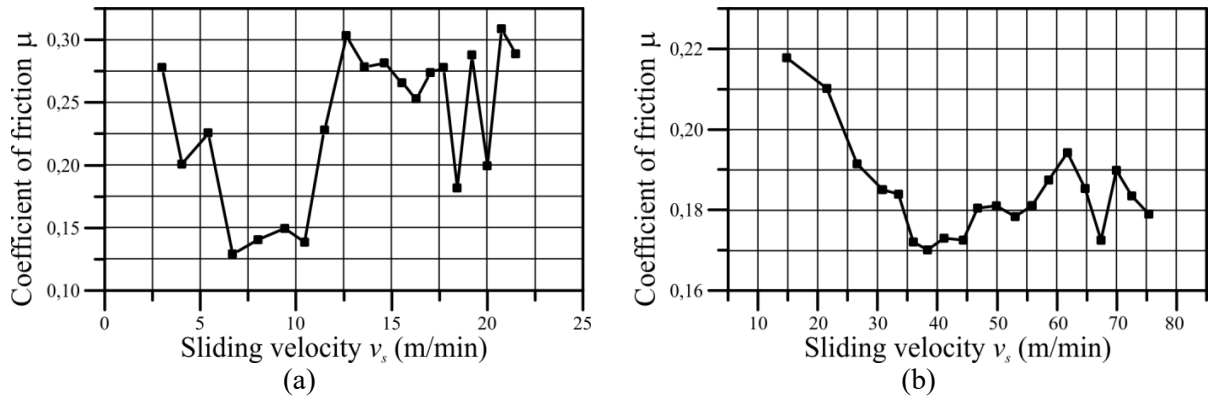

Figure 4. Variations of the friction coefficient in relation to the tool sliding velocity: a – no heat removal applied; b – cooling system applied.

Table 1. Analytical values of friction coefficient.

Tool	Friction coefficient μ			Sliding velocity v_s (m/min)	
	μ_{max}	μ_{min}	μ_{stable}	Prior to steady-state value of friction coefficient v_{stable}	Critical v_{crit}
No heat removal	0.31	0.125	0.13…0.14	7…11	13
With cooling system	0.215	0.165	0.17…0.18	30…55	60

During the nanostructuring burnishing with no heat removal the temperature T_1 of the indenter increased continuously (Figure 5, a) finally reaching ~180 °C at a velocity of 20 m/min; it resulted in

wearing out the indenter tip and putting an end to the operation. Application of the cooling system made it possible to do machining at a velocity of 60 m/min. In this case the temperature T_1 did not exceed 60 °C (Figure 5, b). During the nanostructuring burnishing by the tool with the cooling system temperature T_2 was maintained within 0 and +3 °C.

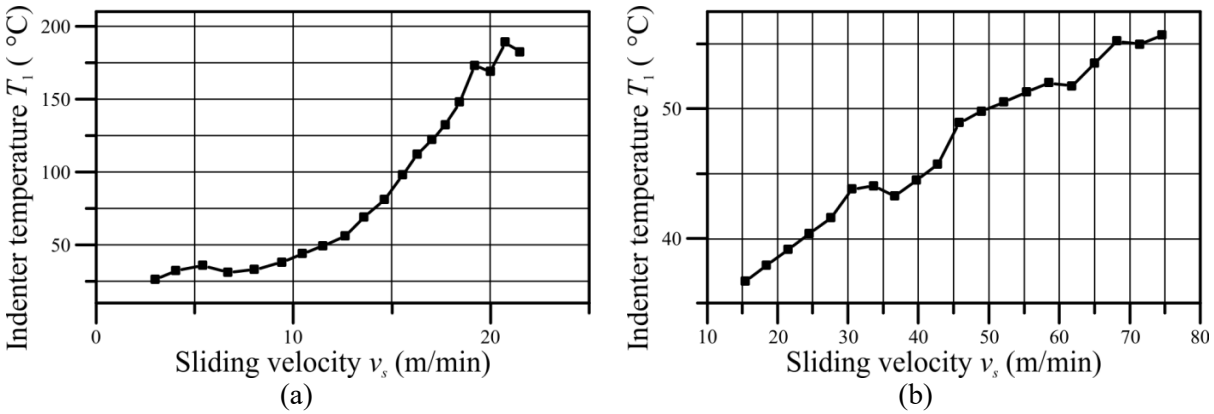

Figure 5. Variations of temperature T_1 at the indenter tip in relation to the tool sliding velocity: a – no heat removal applied; b – cooling system applied.

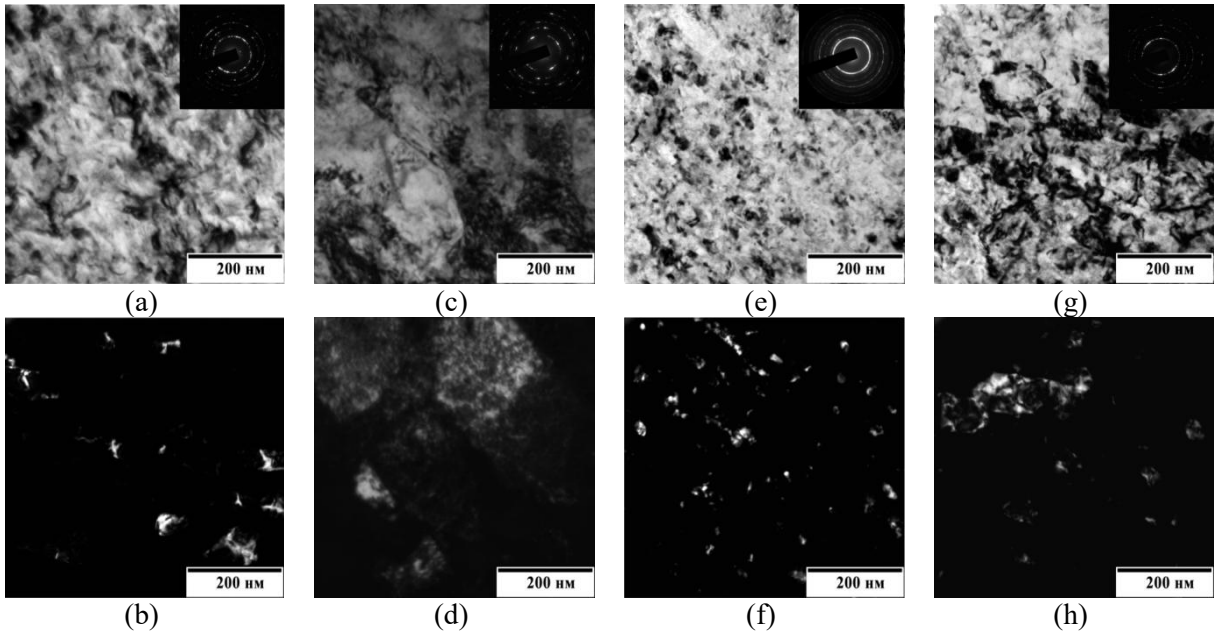

Figure 6. Structure of the surface layer of the sample after nanostructuring burnishing by the tool: a, b and c, d – no heat removal at 10 and 13 m/min, respectively; e, f and g, h – with a cooling system at 45 and 60 m/min.

3.2. Microstructure

TEM was done making use of foils made from the areas of the surface layer corresponding to the middle and boundaries in the range of a stable friction coefficient. It was determined that a nanocrystalline structure forms in the surface layer without losing shear stability when burnishing is done with no heat removal at a velocity below 15 m/min (Figure 6, a and b) and with the cooling system at a velocity below 65 m/min (Figure 6, c and d). High dispersion of the structure is manifested by a circular pattern of α'-phase microdiffraction with a pronounced azimuthal reflection diffusion and

a large number of nanocrystallites measuring 20…80 nm in the dark-field images (figure 6, a, b and e, f).

After nanostructuring burnishing had been completed, two zones were distinguished in the surface layer based on the SEM crossection (Figure 7). The material in zone 1 can be characterized as nanostructured. In zone 2 plastic deformation has a wave shaped pattern with localized shear bands, however, its magnitude is not sufficient for generating a nanostructure. After reaching the velocity v_s=15 m/min with no heat removal the material of the surface layer loses shear stability and is finally destroyed.

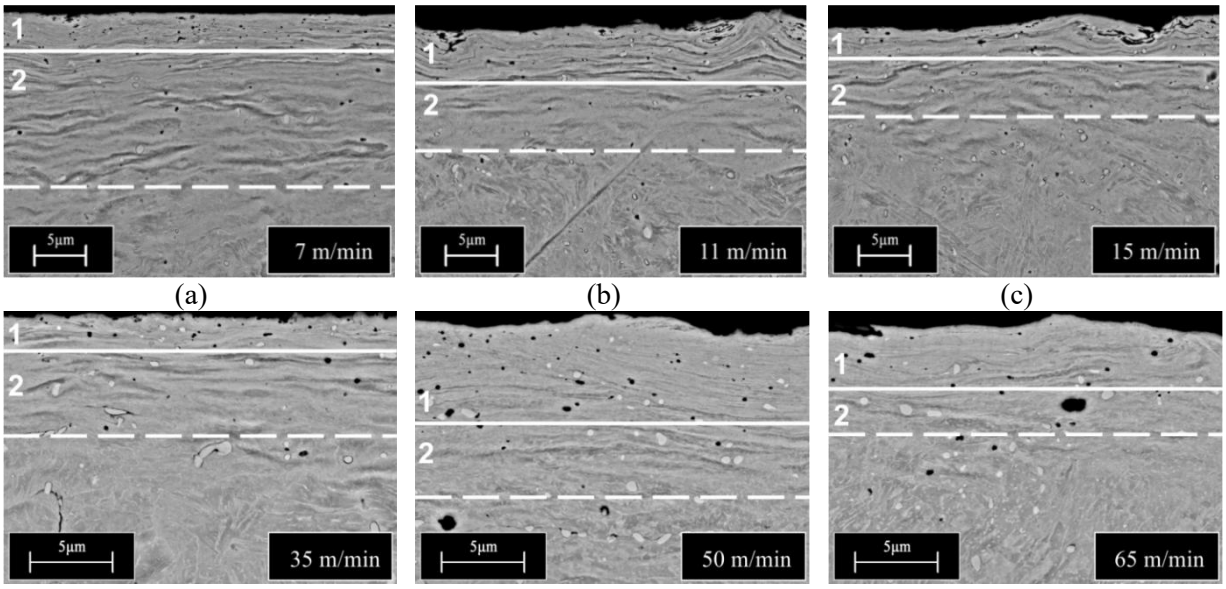

Figure 7. SEM of the surface layer after nanostructuring burnishing with a tool with no heat removal (a, b, c) and with a tool equipped with a cooling system (d, e, f).

SEM images of the surface layer after nanostructuring burnishing in the BSE mode show dark zones, which can identified as pores. The number of pores in zone 2 is lower than in zone 1; however, their size is significantly larger. The biggest pores, some reaching a size of 1 μm, appear when burnishing is done by the tool with the cooling system at a velocity of 45 m/min and above this value. It proves that zone 2 was heated up to a high temperature. In addition to the pores, the modified layer contains light precipitates of circular shape. When the sliding velocity of the indenter is below critical, these precipitates are predominantly in zone 2. At the same time, as the velocity is increased above its critical value, they are also present in zone 1.

When burnishing is done with no heat removal at a sliding velocity of 7 m/min and a coefficient of friction of 0.135, the thickness in zone 1 is 1.5…2 μm (Figure 7, a), while in zone 2 it is 10…11 μm. In zone 2 there are pores, their size being 0.2…0.9 μm. Increasing the velocity to 11 m/min results in evolution of microcracks, elongated in the direction of the indenter feed (Figure 7, b). Meanwhile, the thickness in zone 1 goes up and reaches 4…5 μm, and in zone 2 it goes down and amounts to 7…8 μm. When the sliding velocity is above 11 m/min, light precipitates measuring from 0.2 to 1.3 μm appear in zones 1 and 2; also, microcracks emerge reaching the surface (Figure 7, c). Increasing the velocity from 15 to 20 m/min led to extreme wear of the indenter and deterioration of the surface.

When burnishing is done by the tool equipped with the cooling system at a sliding velocity of 35 m/min and a friction coefficient of 0.165, the thickness in zones 1 and 2 is 1…1.5 μm and 5…6 μm, respectively (Figure 7, d). In zone 2 some light precipitates are as big as 2 μm. If the velocity is raised to 50 m/min and $\mu \approx 0.18$ is obtained, the thickness in zone 1 increases to 5…6 μm,

while in zone 2 it reaches 8…9 μm (Figure 7, e). In zone 2 there appear light precipitates, their size reaching 1.3 μm. When the sliding velocity is 65 m/min and the coefficient of friction is 0.17, the thickness in zone 1 and 2 turns out to be smaller, it goes down to 2…3 μm and 5…6 μm (Figure 7, f). Large light precipitates, their sizes reaching 1.4 μm, emerge in zone 2 and in the boundary of zone 1.

EBSD analysis of the structure in the surface layer (Figure 8) after nanostructuring burnishing had been completed revealed that the light precipitates are a phase with a FCC crystal lattice, i.e. austenite. It can be presumed that in the process of burnishing the surface layer material was heated up to the critical temperature A_{c3} (≥900 °C), which corresponds to the phase recrystallization $\alpha' \rightarrow \gamma$ followed by a recurrence of martensitic transformation $\gamma \rightarrow \alpha'$ as a result of cooling to the temperature A_{r3} (660 °C). Taking into consideration that the major phase in the subsurface layer is martensite, there are sufficient grounds to say that the circular austenitic precipitates evolved due to short spells when the temperature of the material was 660…900 °C. In this intercritical temperature range when ferrite and austenite can coexist, pores and particles of austenite coagulated owing to intensive diffusion of carbon vacancies and atoms in ferrite. Vigorous plastic deformation of the material could also contribute to stabilizing areas of austenite in zone 2.

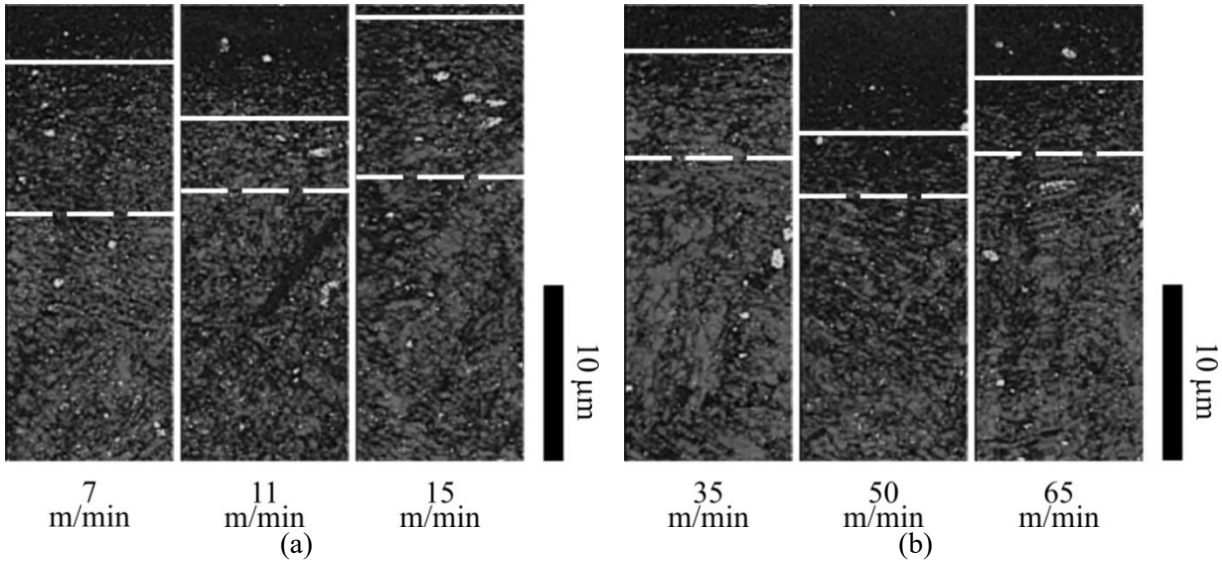

Figure 8. EBSD analysis map shows a microstructure with superimposed phase distribution (Mapping Band Contrast+Phase Contrast) in the surface layer of the sample after nanostructuring burnishing with the tool without heat removal (a) and with an indenter cooling system (b).

EBSD analysis was performed to correlate the phase composition in the material, which is being deformed, and the stability of the evolving nanostructured layer while the burnishing rate was increased. The maps of the microstructure (Figure 8) in the surface layer show selected zones that correspond to zones 1 and 2 marked in the SEM images (Figure 7).

The light precipitates, which can be observed in the marked zones and the main matrix of the deformed material, are identified as γ-phase grains. It can be presumed that emergence and growth of the austenite grains are related to the material under deformation reaching the phase transition temperature (~860 °C) and dynamic recrystallization.

Formation and growth of the γ-phase grains in zone 1 begins in the case of burnishing with the tool with no heat removal as soon as the velocity reaches 11 m/min. If the velocity grows to 15 m/min, relatively large austenite grains measuring 0.6…1.3 μm (Figure 8, a) evolve in the nanostructured layer. Hardly any γ-phase grains can be observed in the nanostructured layer when the sliding velocity of the indenter with the cooling system is increased up to 50 m/min. But when the velocity goes up from 50 to 65 m/min (Figure 8, b), in zone 1 considerable austenite grain growth commences.

Therefore, emergence of the γ-phase grains in the material going through deformation in the nanostructured layer can be considered as a practical criterion to determine the maximum permissible (critical) sliding velocity for nanostructuring burnishing. Thus, permissible sliding velocities for burnishing with the tool with no heat removal and with the indenter cooling system are the velocities equal to 11 and 50 m/min respectively.

3.3. Surface roughness and microharndess

Emergence of large γ-phase grains in the nanostructured layer also produces a detrimental effect on the roughness of the surface microprofile. Optical 3D-profilometry showed that with permissible sliding velocities of the indenter with and without heat removal a stable friction coefficient, μ= 0.17…0.18 and 0.13…0.14 respectively, is ensured and a minimum roughness of Ra≈180…220 nm is obtained (Figure 9, a and c).

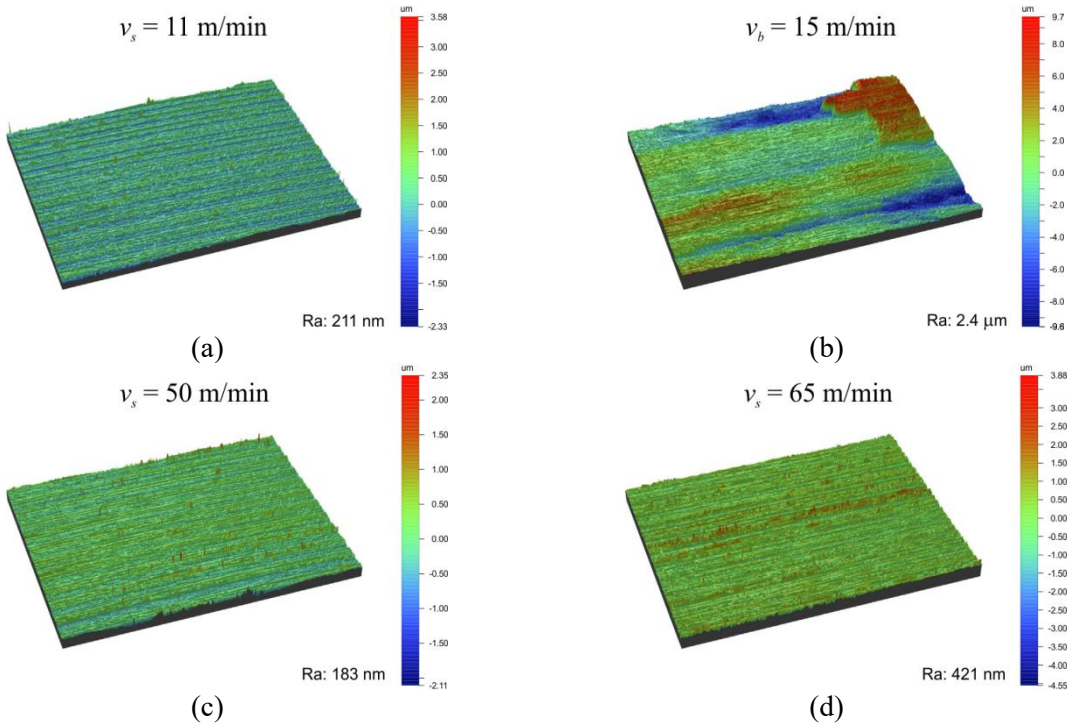

Figure 9. Microprofile of the surface after nanostructuring burnishing without heat removal (a, b) and with a cooling system (c, d).

At sliding velocities beyond permissible values large γ-phase grains form in the nanostructured layer and the roughness grows to Ra≈2.4 μm (Figure 9, b) and Ra≈0.42 μm (Figure 9, d) respectively in both cases, when burnishing with no heat removal and with the cooling system. There emerge local tears in the material of the nanostructured layer as the growth of γ-phase recrystallized grains might be accompanied by an evolving mechanism of peel-off wear. An analogous mechanism of wearing counterbodies was studied in the research (Chen et al., 2014).

Formation of relatively large γ-phase grains in the subsurface layer and nanostructured layer can also be considered to be the cause for the lower microhardness of the surface (Figure 10, a and b) because recrystallized grains have by far lower hardness compared to that of the nanocrystall martensite structure. The maximum microhardness that can be achieved in the case of burnishing without heat removal is 1100…1150 $HV_{0.5}$; in the case when the cooling system is applied, it is 1100…1210 $HV_{0.5}$.

The established character of changes to the microhardness after the critical sliding velocity is reached when burnishing without heat removal and when burnishing with a cooling system suggests

that the most favorable conditions for nanostructuring exist at the temperature of the material under deformation close to the temperature of the phase transition α'→γ. However, to support this suggestion separate research is needed.

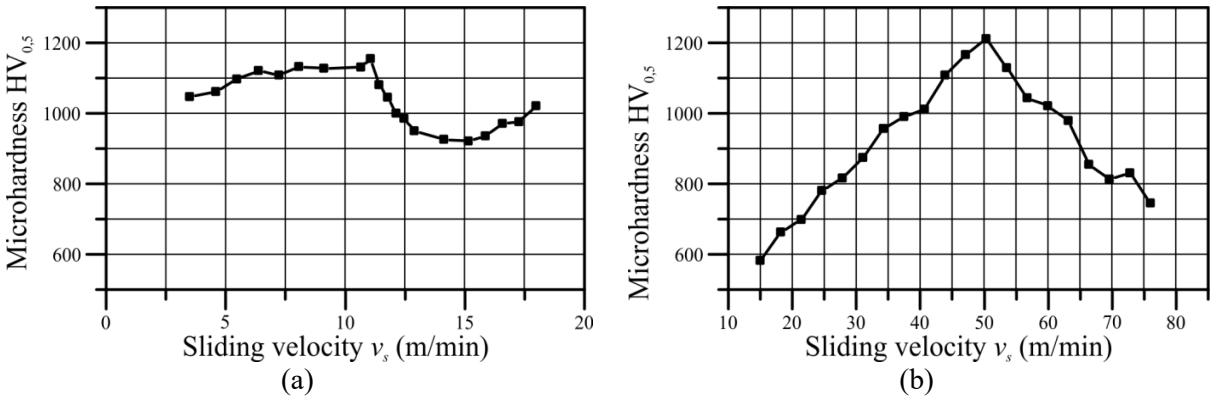

Figure 10. Correlations between the microhardness of the surface layer and sliding velocity: a – by the tool with no heat removal; b – by the tool with a cooling system.

4. Conclusions

a) The extent of dispersion of the surface layer structure to obtain nanocrystallites is to a large extent dependent on the stability and value of the friction coefficient.

b) A homogenous nanostructure containing 20…80 nm crystallites when burnishing the X20Cr13 steel with a tool with no heat removal is obtained provided the sliding velocity range from 7 to 11 m/min and the friction coefficient stays at μ=0.13…0.14. Application of a cooling system based on a Peltier TEC to maintain the temperature of the coolant within 0…+3 °C and the indenter temperature below 60 °C makes it possible to raise the sliding velocity to 65 m/min. Stabilizing the friction coefficient within 0.17…0.18 contributes to increasing the thickness of the nanostructured layer from 1.5…2 μm to 5…6 μm.

c) Emergence of the recrystallized γ-phase attributed to the intense heating of the friction contact can be applicable as a practical criterion to determine the permissible sliding velocity of the indenter.

References

[1] Kuznetsov V P, Smolin I Y, Dmitriev A I, Tarasov S Y, Gorgots V G 2016 *Surf. and Coat. Technol.* **285** 171
[2] Kuznetsov V P, Tarasov S Y, Dmitriev A I, 2015 *J. of Mater. Process. Technol.* **217** 327
[3] Korzynski M, Pacana A, Cwanek J 2009 *Surf. and Coat. Technol.* **203** 1670
[4] Kuznetsov V P, Makarov A V, Psakhie S G, Savrai R A, Malygina I Y, Davydova N A 2014 *Phys Mesomech.* **17** 250
[5] Rabinowicz E, Imai M 1963 *Wear* **6** 407
[6] Bonnet C, Valiorgue F, Rech J, Claudin C, Hamdi H, Bergheau J M, Gilles P 2008 *Int. J. of Mach. Tools and Manuf.* **48** 1211
[7] Ben Abdelali H, Claudin C, Rech J, Ben Salem W, Kapsa P, Dogui A 2012 *Wear, Tribol. in Manuf. Process.* **286–287** 108
[8] McQueen H J, Jonas J J 1985 *J. Appl. Metalwork.* **3** 410
[9] Pu Z, Song G-L, Yang S, Jr O W D, Puleo D A, Jawahir I S 2011 *Magnes. Technol.* **2011** 513
[10] Kuznetsov V P, Skorobogatov A S, Gorgots V G, Yurovskikh A S 2016 *IOP Conf. Ser.: Mater. Sci. Eng.* **124** 12127 https://doi.org/10.1088/1757-899X/124/1/012127